Evolution with private resources reverses some changes from long-term evolution with public resources

Katrina van Raay[1,2], Sergey Stolyar[2,3], Jordana Sevigny[1,2], Jeremy A. Draghi[4], Richard E. Lenski[2,5], Christopher J. Marx[2,3,6,7], Benjamin Kerr[1,2], Luis Zaman[2,8]

1. Department of Biology, University of Washington, Seattle, WA;

2. BEACON Center for the Study of Evolution in Action, Michigan State University, East Lansing, MI;

3. Department of Biological Sciences, University of Idaho, Moscow, ID;

4. Department of Biological Sciences, Virginia Tech, Blacksburg, VA;

5. Department of Microbiology and Molecular Sciences; Michigan State University, East Lansing, MI;

6. Institute for Modeling Collaboration and Innovation, University of Idaho, Moscow, ID;

7. Institute for Bioinformatics and Evolutionary Studies, University of Idaho, Moscow, ID;

8. Department of Ecology and Evolutionary Biology, and Center for the Study of Complex Systems, University of Michigan, Ann Arbor, MI.

Abstract

A population under selection to improve one trait may evolve a sub-optimal state for another trait due to tradeoffs and other evolutionary constraints. How this evolution affects the capacity of a population to adapt when conditions change to favor the second trait is an open question. We investigated this question using isolates from a lineage spanning 60,000 generations of the Long-Term Evolution Experiment (LTEE) with *Escherichia coli*, where cells have access to a shared pool of resources, and have evolved increased competitive ability and a concomitant reduction in numerical yield. Using media-in oil emulsions we shifted the focus of selection to numerical yield, where cells grew in isolated patches with private resources. We found that the time spent evolving under shared resources did not affect the ability to re-evolve toward higher numerical yield. The evolution of numerical yield commonly occurred through mutations in the phosphoenolpyruvate phosphotransferase system. These mutants exhibit slower uptake of glucose, making them poorer competitors for public resources, and produce smaller cells that release less carbon as overflow metabolites. Our results demonstrate that mutations that were not part of adaptation under one selective regime may enable access to ancestral phenotypes when selection changes to favor evolutionary reversion.

Keywords: evolution, tradeoffs, constraints, metabolism

Introduction

The history of life has been inextricably shaped by evolutionary constraints. Given phenotypic trade-offs, an organism cannot simultaneously optimize two traits with respect to fitness (Agrawal et al. 2010; Stearns 1989). Thus, a population under strong selection to improve one trait may evolve a sub-optimal state for another trait. More generally, pleiotropy means that mutations in one gene affect multiple traits simultaneously (Pavličev & Cheverud, 2015), and antagonistic pleiotropy occurs when mutations are beneficial for one trait but detrimental for another. While there is a rich literature on evolutionary tradeoffs (Beardmore et al. 2011; Gounand et al. 2016; Guillaume & Otto, 2012) and antagonistic pleiotropy (Rose, 1982; Rose, 1985), there has been less attention given to how the evolutionary history of a lineage under selection for one trait affects its subsequent trajectory when selection shifts to favor a second trait that trades off with the first (but see Ostrowski et al. 2015; Teotónio & Rose, 2000; Travisano & Lenski, 1996; Velicer, 1999).

To understand how previous adaptation might affect future evolution, let us imagine a population under long-term selection for one trait that trades off with a second trait (Figure 1a). For simplicity, we assume higher values of each trait correspond to higher fitness when under selection. Long-term improvement in the favored trait (trait 1 in Figure 1a) occurs along with concomitant decreases in the second trait (trait 2). If selection shifted to favoring trait 2, how would the duration of history evolving under selection for trait 1 affect future evolution (Figure 1b)? There are at least two plausible hypotheses about how that duration would influence the rate of adaptation. The "Mutational Access" hypothesis (Figure 1c) posits that populations that spent more time under selection for trait 1 have fewer available mutations that would improve fitness by increasing trait 2 (i.e., the "late descendant" compared to the "intermediate descendant" in Figure

1a). If so, then this would lead to a *lower* rate of adaptation for the late descendant than for the intermediate one when trait 2 is favored. This mutational limitation could result from the necessity of compensating for (or reverting) more mutational steps; alternatively, it might occur if mutations increasing trait 2 become increasingly deleterious over time due to the entrenchment of trait 1 (Schank & Wimsatt, 2011; Shah et al. 2015). The "Strength of Selection" hypothesis (Figure 1d), by contrast, suggests that the intermediate and late descendants have equal access to mutations improving trait 2, but the selective benefits for the late descendant are greater due to the relatively larger changes in fitness upon improvement (Barrick et al. 2010; Chou et al. 2011). Under this hypothesis, the rate of adaptation is predicted to be *higher* for the late descendant.

If adaptation is possible under selection for trait 2, then we expect a return towards the progenitor's value of that trait. Does this phenotypic return occur by "rediscovering" the ancestral genetic and mechanistic underpinnings of the second trait (Levin et al. 1997; Pennings et al. 2020)? This rediscovery could occur by reverting key mutations, or by otherwise returning to the regulatory, physiological, or metabolic states that enabled the progenitor's phenotype. Indeed, the mechanisms that underly a return to the ancestral state (e.g., Figures 1b-d) might differ depending on whether evolution is initiated with intermediate or late descendants.

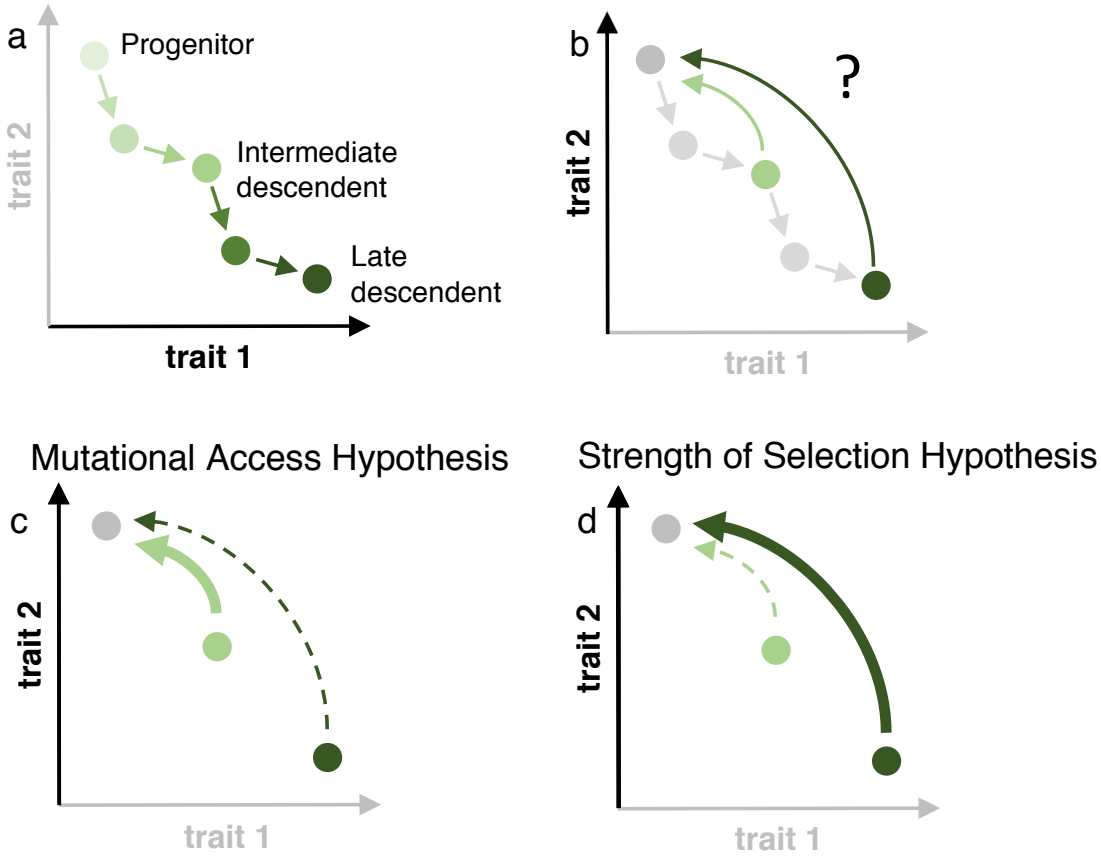

Figure 1: Evolutionary trajectories and alternative hypotheses. a) A population evolves under direct selection for one trait (trait 1, bolded axis). A higher value along either axis indicates an improvement in that trait under selection. Each circle represents a genotype in an evolutionary line of descent. We focus on three genotypes along an evolutionary trajectory: the progenitor, an intermediate descendent, and a late descendant. b) Selection is relaxed for trait 1 and strengthened for trait 2 (bolded axis). The curved arrow represents the transition of a population with descendent traits towards traits that resemble the progenitor when selection acts on trait 2. Whether, how fast, and by what mechanisms this transition occurs are the main questions addressed in this paper. c) Mutational access hypothesis. Intermediate (light green) and late (dark green) descendants are shown after selection is relaxed on trait 1 and strengthened on trait 2. The width of arrows pointing from each descendent towards the progenitor indicates the rate of change. The thick arrow from the intermediate descendent denotes a faster return to the progenitor phenotype than the dashed arrow from the late descendent. Under this hypothesis, the late descendent is either mutationally further from the progenitor state or the mutational options to revert to the progenitor phenotype are more costly due to entrenchment. d) Strength of selection hypothesis. Intermediate (light green) and late (dark green) descendants are shown when selection flips from favoring trait 1 to trait 2. The width of arrows pointing from each descendent towards the progenitor indicates the relative strength of selection. The thick arrow from the late descendent indicates stronger selection favoring a mutation that restores the ancestral phenotype, and thus a faster response, than for the same mutation in the intermediate descendant (dashed arrow). Under this hypothesis, both descendants have the same mutational access to various positions in phenotype space.

Here we present a realization of the thought experiment in Figure 1, in which we test how the length of time that populations of *Escherichia coli* had been selected for faster growth affects their future adaptation in a novel environment that favors increased numerical yield (i.e., number of cells per concentration of substrate added). To do so, we take advantage of the Long-Term Evolution Experiment (LTEE), in which 12 replicate populations of *E. coli* have been evolving for over 70,000 generations in a relatively simple environment (Lenski 2017; Vasi et al. 1994; Wiser et al. 2013). Periodic samples from each line have been frozen in suspended animation, so that the "progenitor," "intermediate descendant," and "late descendant" are available by reviving samples from this living fossil record. The well-stirred, unstructured environment maintains a single, public pool of resources for the population and thus favors rapid growth, above all else (Vasi et al. 1994, Novak et al. 2006). Furthermore, there is no expectation of direct selection for either numerical yield or metabolic yield (proportion of carbon in the substrate that is incorporated into biomass). In an unstructured environment, a mutant that consumes resources more slowly but efficiently is disadvantaged, because a faster-growing but less-efficient competitor can deplete the shared resources in the meantime. Instead, a mutant that grows faster has an advantage in an unstructured environment, even if it leads to a reduction in the population's numerical yield, metabolic yield, or both.

The outcomes in the LTEE are slightly more complicated, and they are mediated in part by changes to a third trait: cell size (Mongold & Lenski 1996). All of the LTEE lineages show increases in competitive ability relative to their common ancestor, while simultaneously having lower numerical yields (Vasi et al. 1994, Wiser et al. 2013). The reductions in numerical yield result from the evolution of much larger individual cells (Lenski & Travisano 1994, Vasi et al. 1994, Grant et al. 2021). In many bacteria, increased cell size is a physiological response to

127 increased growth rate (Johnston et al. 1979; Pierucci, 1978). In addition, some mutations in
128 bacteria affect both growth and cell size or shape (Monds et al. 2014, Yulo & Hendrickson 2019).
129 Therefore, it is reasonable to expect that selection for faster growth has led to larger cells and, as
130 a pleiotropic consequence, decreased numerical yield.

131 These evolutionary changes also extend to metabolic yield—the efficiency with which
132 carbon sources are converted into biomass. During exponential growth on glucose, when most of
133 the doublings occur during the LTEE daily cycle, direct measurements of metabolic yield through
134 central metabolism show a small (but significant) decrease in the evolved populations. The
135 excretion of acetate, an overflow metabolite, also increased by about 50% in the LTEE (Harcombe
136 et al. 2013). Similar to the case with cell size, some loci with beneficial mutations in the LTEE
137 lineages are known to affect acetate metabolism (Quandt et al. 2015); it is also known that rapid
138 growth *per se* leads to increased overflow metabolite production in *E. coli* (Barrick & Lenski 2009;
139 Farmer & Jones 1976). This situation is further complicated, however, by the finding that the LTEE
140 populations have evolved increased total biomass when measured after a full 24-hour growth cycle
141 (Lenski & Mongold 2000, Novak et al. 2006). While the increase might be caused in part by a
142 change in biomass composition, it also reflects an increased ability to use excreted metabolites
143 after the glucose has been depleted. Indeed, the evolved LTEE strains have increased their ability
144 to grow on acetate, as well as to grow on other overflow metabolites that the LTEE ancestor could
145 not use (Leiby & Marx, 2014). Although there was no direct advantage to increased biomass in a
146 well-mixed environment, nonetheless biomass increased alongside faster growth in the LTEE. This
147 constellation of changes can be understood by considering that, in the novel environment of the
148 LTEE, the ancestral strain was likely far from the trade-off front between growth rate and total
149 biomass, leaving room for improvements in both trats (Novak et al. 2006).

Now consider what might happen if the bacteria that previously evolved in the LTEE moved to and evolved in a structured environment that was otherwise similar to the unstructured LTEE environment. By distributing a transplanted population into many isolated 'patches,' each seeded by a single cell, any resources saved by growing more efficiently would accrue disproportionately to cells with the same genotype, which would effectively eliminate resource competition. Now imagine that the cells in these patches were periodically pooled, diluted distributed as single founders over a new set of empty patches. In that case, selection would favor increased numerical yield since each individual cell is a potential propagule able to establish a new subpopulation. Increased numerical yield could be achieved by increasing the metabolic yield, by producing smaller individual cells, or perhaps by some combination of these changes. In this way, selection shifts to favor numerical yield over competitive ability for shared resources (accomplishing the transformation from Figure 1a to Figure 1b in our thought experiment).

In our study, we achieve this shift by propagating cells in water-in-oil emulsions comprised of millions of aqueous media-filled droplets surrounded by an oil phase (Figure 2) (Bachmann et al. 2013). If a population of cells is diluted sufficiently before creation of the emulsion, then each cell will usually be the sole occupant of a droplet. In such a case, barring mutation, there is no competition between genotypes for resources, as each cell (and its progeny) has access to a private resource supply demarcated by the droplet. If growth of isolated cells inside droplets proceeds for sufficient time to exhaust the substrate and is followed by demulsification, dilution, and redistribution into droplets across successive transfers (as in Figure 2a), then those genotypes that produce *more* cells (rather than the fastest-growing cells) will have an advantage. Indeed, prior experiments have demonstrated that various forms of isolation can favor numerical yield at the

172 expense of competitive ability in several different biological systems (Bachmann et al. 2013;
173 Eshelman et al. 2010; Kerr et al. 2006; van Tatenhove-Pel et al. 2021).

174 Here, we instantiate the thought experiment of Figure 1 by considering two bacterial traits:
175 competitive ability (the relative increase in proportion of a focal strain when competing with
176 another strain for shared resources) and numerical yield (the absolute number of cells produced by
177 a focal strain when resources are not shared). We focus on a single LTEE lineage in order to
178 explore how previous selection for one trait (competitive ability) affects the tempo and mode of
179 evolution under selection for a second trait (numerical yield) in the presence of a phenotypic
180 tradeoff. We probe how the length of time adapting to the well-mixed LTEE regime affects the
181 ability of a population to adapt under the new emulsion condition. We examine whether increases
182 in numerical yield during growth with private resources come with associated decreases in
183 competitive ability for shared resources, and whether they are achieved through changes in
184 metabolic yield and associated overflow metabolite production, decreases in cell size, or by both
185 factors. Finally, by determining the nature and number of mutations that occurred, we can
186 investigate whether any evolutionary reversions to the ancestral phenotypes were caused by
187 changes in the same loci/processes that were implicated in the evolution of fast growth in the
188 original LTEE environment.

189

190 ## Methods

191 *Strains*

192 All experiments were founded with *E. coli* B isolates that came from the Ara–5 lineage in the
193 LTEE. The isolates used in our experiment came from 0 generations (the founder of the LTEE),
194 20,000 generations, and 60,000 generations of evolution in the LTEE (Table S1; hereafter called

195 0K, 20K, and 60K, respectively). The 0K isolate is the ultimate progenitor of the 20K and 60K
196 isolates in the context of the LTEE. However, because we conduct evolution experiments in the
197 emulsion system with these three strains, we will refer to these LTEE isolates as the "0K emulsion
198 ancestor", the "20K emulsion ancestor", and the "60K emulsion ancestor".
199
200 *Emulsion evolution experiment*
201 Following the pioneering work of Bachmann et al. (2013), we propagated three replicate
202 cultures founded by each of the three LTEE isolates (the emulsion ancestors) under selection for
203 increased numerical yield by using water-in-oil emulsions for 100 transfers. This method (see
204 below) creates millions of media-filled, picoliter-sized droplets surrounded by an oil phase, in
205 which bacterial cells in one droplet are isolated from those in others (Figure 2). Emulsions were
206 set up in 1.5-ml Eppendorf conical microcentrifuge tubes, and they were incubated at 37 °C
207 without shaking.
208 In order to select for increased numerical yield, we diluted the bacterial culture before
209 setting up the emulsions, such that 90% of occupied droplets would contain only 1 cell at the
210 beginning of each transfer cycle. We subsequently showed that occupied droplets had an average
211 of 1.12 cells (see Supplementary section *Calculating Droplet Statistics*). Bacteria were allowed to
212 grow and divide in droplets for 24 hours, after which the droplets were broken with 1*H*,1*H*,2*H*,2*H*-
213 perfluoro-1-octanol, releasing all the cells into a common pool. A fraction of the cells from this
214 pool were immediately used to initiate the next transfer (see Figure 2a). Because of the level of
215 dilution before emulsification, lineages from this treatment have evolved in "private droplets" (see
216 Figure 2c). This treatment was continued for 100 transfers.
217

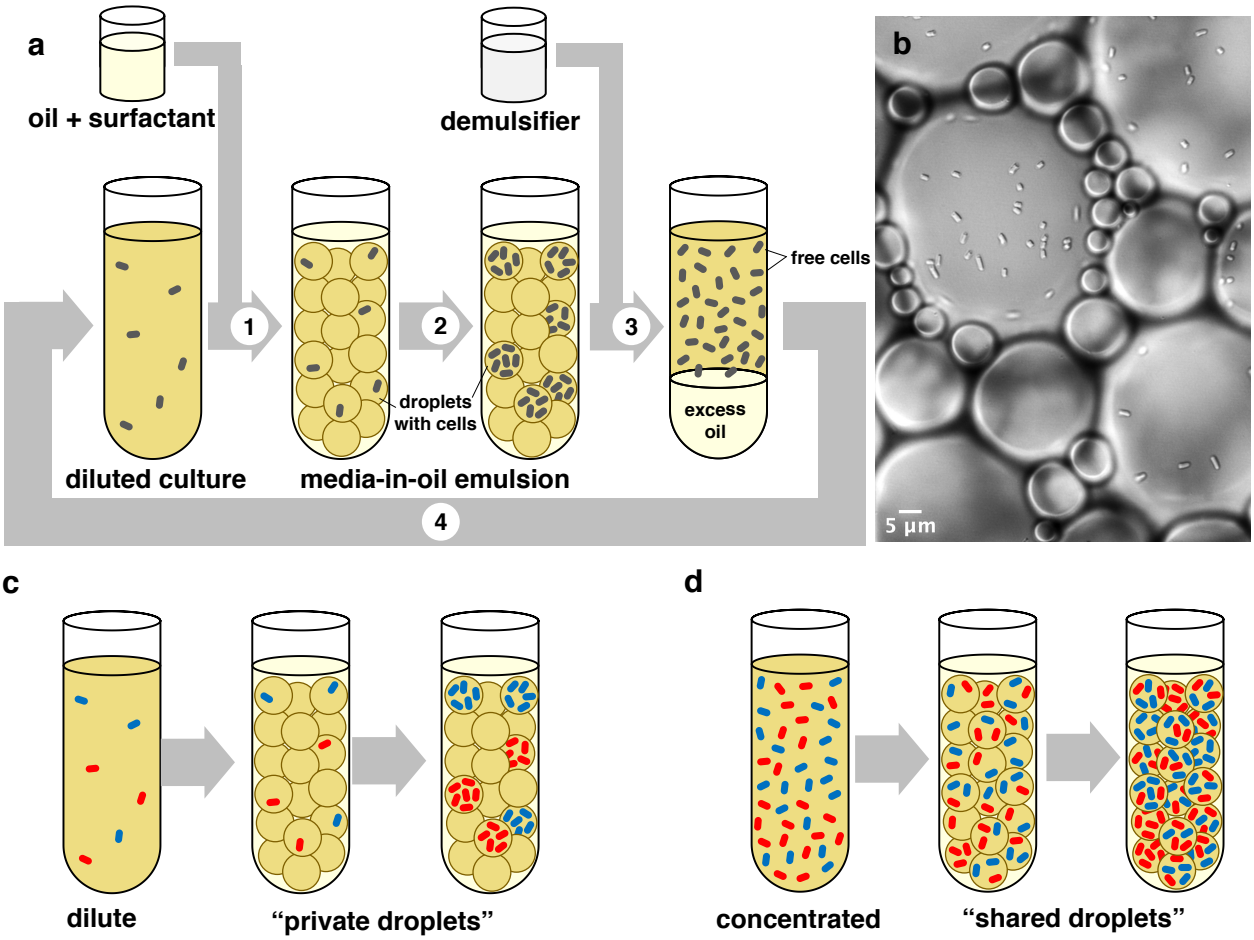

Figure 2: a) Schematic of transfer protocol: 1. A mixture of oil and surfactant is added to a diluted culture of bacteria in growth media and vortexed to form millions of droplets, 2. Bacteria in the emulsion are incubated to allow subpopulation growth within the droplets, 3. After overnight growth, a demulsifier is added to break the emulsion and resuspend the bacteria, 4. The free cells are diluted into fresh media and the cycle is repeated, **b)** Micrograph of bacteria growing in emulsion droplets, **c)** Schematic of inoculation and growth for private droplets, **d)** Schematic of inoculation and growth for shared droplets. For parts c and d, the two colors of bacterial cells represent distinct genotypes.

To control for any effects of growing in emulsions, we also propagated three replicate cultures founded by each LTEE isolate for 100 transfers under higher starting-density conditions, in which each occupied droplet had almost 3 cells on average (see Supplementary section

Calculating Droplet Statistics). We predicted that we would not observe evolution towards increased numerical yield in this "shared-droplet" treatment (see Figure 2d).

During the evolution experiment, the cell density of freshly broken emulsions was measured with a FilterMax F5 Multi-Mode Microplate Reader (Molecular Devices) after 24 hours. Briefly, we pipetted 150 µl of overnight culture from a broken emulsion into a flat-bottom 96-well microtiter plate, and we recorded an OD_{595} reading. This reading was then used to estimate cell density using a calibration curve giving the relationship between OD_{595} and CFU/ml, which was established in prior experiments. Cultures were then diluted to 2×10^6 CFU/ml for the private droplet treatment and 5×10^7 CFU/ml for the shared droplet treatment. Emulsions were created by adding 200 µl of a mixture of 9 parts Novec 7500 HFE to 1 part Pico-surf (5% (w/w)) to 300 µl of diluted culture in the growth medium DM1000 in 1.5 ml Eppendorf tubes, and vortexing at maximum speed for 2 minutes. DM1000 contains 1000 mg/l of glucose, and it was used instead of the DM25 (25 mg/l glucose) used in the LTEE because DM1000 exhibited clearer differences between the 0K and 60K samples in terms of numerical yield and competitive ability than DM25 in pilot experiments.

Single-colony isolates were picked from each population at the end of our evolution experiment (after transfer 100) and frozen at -80 °C as 20% v/v glycerol stocks. We refer to these evolved isolates as "emulsion descendants." Two loci previously shown to distinguish the 0K, 20K, and 60K ancestors were Sanger sequenced for each isolate to confirm the intended derivation of the isolates. We detected within-experiment contamination via Sanger and subsequent whole-genome sequencing in 4 of the 18 emulsion descendants, so these populations were dropped from our analysis. The complete genomes of the remaining 14 strains (8 private droplet, 6 shared droplet) were sequenced and analyzed, and the 6 isolates of private-droplet descendants that had

253 mutations were used for further analysis. For the shared droplet treatment, one descendent was
254 randomly chosen from each lineage to be assessed in the phenotypic assays (3 isolates).
255
256 *Competition assays*
257 Using the frozen samples of the emulsion ancestors (0K, 20K, and 60K) and their emulsion
258 descendants from the private and shared droplet treatments, we assessed the relative competitive
259 abilities of all of our strains. The emulsion descendants competed against a common marked strain
260 (equivalent to our 0K emulsion ancestor) in shared droplet conditions. We used a neutral marker
261 (a point mutation in the *araA* gene) to distinguish the focal and common competitor strains on
262 tetrazolium-arabinose indicator agar plates.
263 Competitions ran for 3 transfer cycles in emulsions. Competitions were initiated with a 1:1
264 ratio of the focal strain (denoted F) to the common competitor (denoted C). The competitive ability
265 of the focal strain relative to the common competitor ($w(F,C)$) was assessed by calculating a ratio
266 of their realized Malthusian growth rates (Lenski et al. 1991):

267 $$w(F,C) = \frac{\ln \frac{F_{\text{final}}}{F_{\text{initial}}} + \sum_{i=2}^{3} \ln z_i}{\ln \frac{C_{\text{final}}}{C_{\text{initial}}} + \sum_{i=2}^{3} \ln z_i},$$

268 where X_{initial} and X_{final} are the initial (beginning of the first transfer) and final (end of the third
269 transfer) densities, respectively, of strain X (with $X \in \{F, C\}$) and z_i is the factor by which the
270 population is diluted in order to initiate the i^{th} transfer.
271
272 *Genome Sequencing*
273 Single-colony isolates from 14 evolved lines and their 3 ancestors were grown in DM1000
274 and frozen as 20% v/v glycerol stocks at -80 °C. For genome sequencing, cells from these frozen

stocks were reanimated in 5 ml of LB (lysogeny broth). Genomic DNA was extracted using a Qiagen DNEasy kit with 1 ml of overnight culture, following the manufacture's protocol. Library preparation and sequencing for 16 strains was done at the Microbial Genome Sequencing Center (MiGS) at the University of Pittsburgh. One strain (the 0K emulsion ancestor) was sequenced at the University of Washington on Illumina's NextSeq platform and prepped with Illumina Nextera barcodes. Genome sequences had an average of 131X coverage.

Mutations (predicted mutations, unassigned missing coverage, and unassigned new junctions) were called using breseq (Version 0.33.2) (Deatherage & Barrick, 2014) with default parameters. All mutations were confirmed using Integrative Genomics Viewer (Robinson et al. 2011), and four point mutations identified in strains that differed phenotypically from their ancestors in cell size or numerical yield were Sanger sequenced for confirmation (Table S4).

Numerical yield and cell size assays

Populations of each emulsion ancestor and descendant were grown under the shared-droplet conditions over a standard 24-hour growth cycle. We used the shared-droplet emulsions instead of the well-stirred conditions to control for the microenvironmental effects of growing in an emulsion (e.g., oxygen depletion during growth). The final cell number in the 24-hour sample was used as our measure of numerical yield. Cell size was measured as the median cell volume (μm^3) of several thousand cells using a Beckman Coulter MSE 4 instrument.

Metabolic analysis

Supernatants from the yield assays were filtered and stored at -80 °C prior to metabolic analysis. After thawing, samples were analyzed using High Performance Liquid Chromatography

298 (HPLC) on a 20A chromatographic system (Shimadzu) equipped with diode array and refractive
299 index detectors. Samples were eluted with 6 mM H_2SO_4 at a flow rate of 0.6 ml/min from an
300 Aminex HPX 87H organic acid analysis column (300 by 7.8 mm) (BioRad). We recorded the areas
301 for all noticeable peaks associated with detected metabolites (glucose, citrate, acetate, formate, and
302 lactate), and these values were converted to metabolite concentrations (in mM) using organic acid
303 and sugar standards (from BioRad or made in-house). Citrate, an iron chelator present in DM
304 medium, is neither produced nor consumed by these bacterial strains, and it has been shown not to
305 affect the growth of the Ara–5 lineage (Leiby et al. 2012). Thus, citrate was used as an internal
306 control.
307
308 *Analysis of metabolic data*
309 The rates of production for each metabolite are difficult to compare because of differences
310 in the growth rates of the strains. To minimize this potentially confounding factor, we performed
311 linear regression of the concentration of each metabolite against the remaining concentration of
312 glucose. The magnitude of the slope of this relationship estimates the ratio of metabolite
313 produced for each unit of glucose consumed, assuming an approximate equilibrium between the
314 uptake of glucose and the release of metabolites into the medium. As glucose levels drop, however,
315 there is increased uncertainty in the glucose measurements; moreover, as the glucose becomes
316 scarce, the cells may begin to consume the excreted metabolites, which would bias our estimates
317 of the production rates. To avoid these problems, we excluded time-points in the linear regressions
318 for which the mean glucose concentration was below 0.8 mM. We chose this threshold because,
319 at lower concentrations, growth curves showed clear signs of departure from exponential growth.
320 We also excluded the measurements made at t=0 and, instead, we constrained the x-intercept of

the regressions to reflect the known initial concentrations in the media (i.e., 6 mM glucose and none of the overflow metabolites). To estimate how quickly the glucose was consumed, we performed regressions of glucose concentrations against time, using the same criteria for data exclusion. This approach provided a measure of growth rate that was insensitive to differences in cell size across strains.

Results & Discussion

Private-droplet treatment selected for high numerical yield

Our private droplet treatment was designed to minimize local competition between genotypes, thereby focusing selection upon increased numerical yield. To assess whether the emulsion-evolved populations underwent changes in numerical yield, we measured their cell densities, along with those of their ancestors, at the end of 24 hours of growth in the emulsion system. Providing some reassurance that salient features of the LTEE environment are maintained in our emulsion cultures, the decreases in numerical yield seen during the LTEE were also detected in emulsion -- the 20K and 60K ancestors had decreased numerical yield compared to the 0K ancestor (Figure 3, Table S3; $p < 0.01$, unpaired one-tailed t-tests). All 6 private droplet descendants had significantly increased numerical yield (cell number) compared with their direct ancestor (Figure 3, Table S2; BK 433: $p < 0.05$; BK 431, BK 437, BK 438, BK 441, BK 442: $p < 0.01$, unpaired two-tailed t-tests). Our shared-droplet treatment served as control for the private-droplet treatment, allowing local competition between genotypes, while controlling for growth in the emulsion environment. Two of the three shared-droplet descendants had increased numerical yield and one had decreased yield; however, the gains were less than those in the private-droplet treatment, and all three changes were non-significant. Combining the 0K, 20K, and 60K lines, the

344 private-droplet descendants were significantly more productive than the shared-droplet
345 descendants (p=0.039, paired one-tailed t-test; see Supplementary section *Statistical Analysis*).
346 The two evolutionary treatments had different effective population sizes. However, the weaker
347 numerical-yield response in the shared-droplet treatment relative to the private-droplet treatment
348 cannot be explained by the lack of mutational opportunity, because the number of cell divisions
349 per transfer is actually greater in the shared-droplet treatment (see Supplementary section
350 *Calculating Number of Cell Divisions in Droplets)*. Taken together, these data confirm our
351 prediction that the private-droplet treatment exerts stronger selection for increased numerical yield
352 than does the shared-droplet treatment.

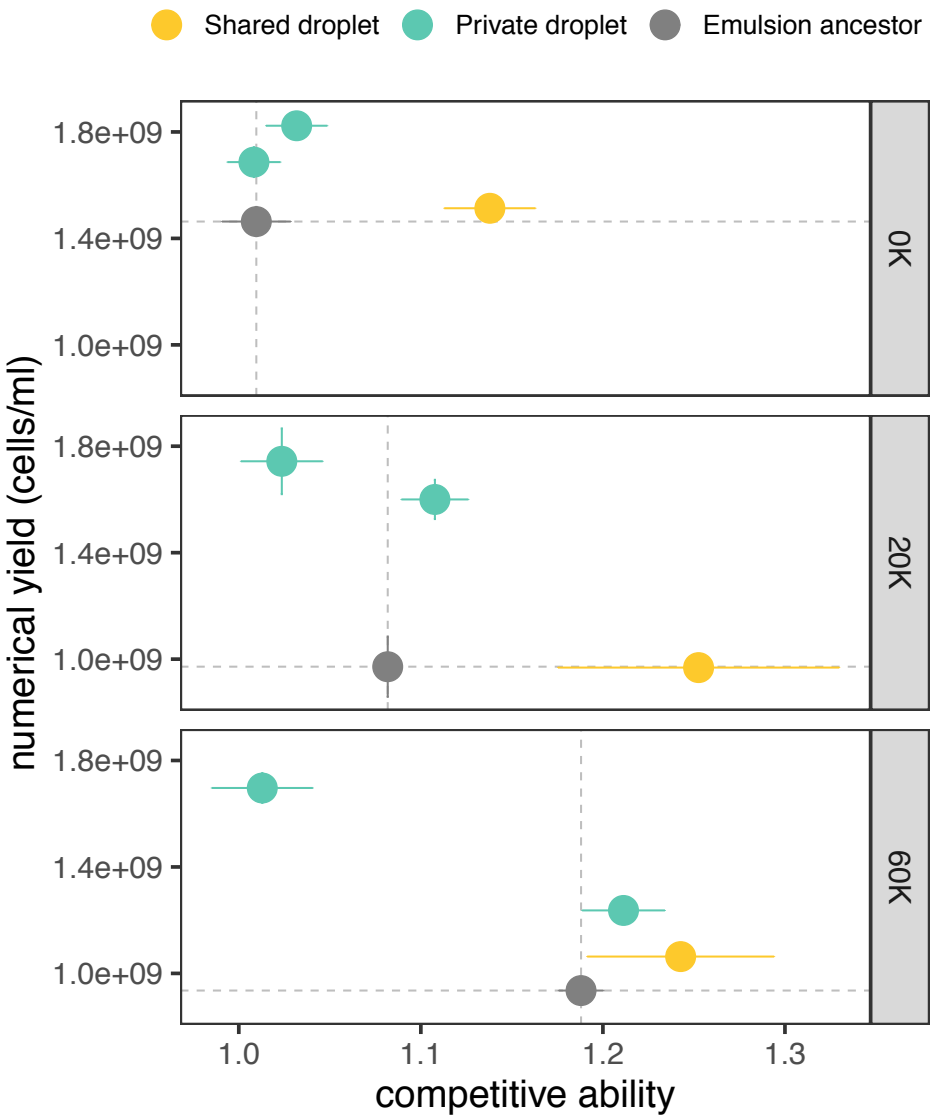

353

354 **Figure 3:** Numerical yield (cell density after the standard 24-hour growth cycle) compared to relative competitive
355 ability, both measured in the emulsion system. Each panel shows strains originating from a single emulsion ancestor
356 (in grey, at right) from the Ara–5 lineage of the LTEE (0, 20,000, and 60,000 generations). Colors indicate emulsion
357 evolution treatments (labels at top). The coordinate positions of each point are the averages of three replicate assays
358 for each phenotypic trait. Error bars show SEM; when they are not visible along either axis, the corresponding SEM
359 is smaller than the symbol itself. Dashed lines show the mean competitive ability and numerical yield of the relevant
360 ancestor.

361

362 In particular, the shared-droplet results demonstrate that the increase in numerical yield in
363 the private-droplet treatment was not simply an evolutionary response to propagation under the
364 emulsion conditions. Instead, these results imply that the initial density within a droplet affects the
365 evolutionary outcome. By reducing competition between genotypes within the private droplets,
366 selection has favored numerical yield.
367
368 *Shared droplet treatment favored competitive ability*
369 When resources are shared, selection for greater competitive ability is expected. To assess
370 competitive ability, a focal strain was paired with a marked version of the 0K ancestor and
371 proportions were tracked under high density emulsion conditions such that resources were shared
372 between competitors. Again, emulsion populations showed consistent results with the batch culture
373 environment used during the LTEE -- the competitive ability of the 20K ancestor was elevated
374 compared to the 0K ancestor, and the 60K ancestor had a further increase over the 20K ancestor
375 (Figure 3,Table S3; $p < 0.05$ unpaired, one-tailed t-tests). Competitive ability increased in all three
376 shared-droplet descendants that we tested (Figure 3). However, the change was significant relative
377 to the corresponding emulsion ancestor only in the case of the line derived from the 0K ancestor
378 (Table S2). Competitive ability also increased in three of the six private-droplet descendants, but
379 none of these increases were significant, and the magnitudes of the increases were smaller than
380 those observed in the shared-droplet treatment. Competitive ability decreased in the other three
381 private-droplet descendants, and the decline was significant in one case (BK 441: $p < 0.01$,
382 unpaired two-tailed t-test). Combining the results from the 0K, 20K, and 60K lines, the shared-
383 droplet descendants were significantly more competitive than the private-droplet descendants ($p =$
384 0.038, paired one-tailed t-test; see Supplementary section *Statistical Analysis*). Overall, these

385 results support our prediction that starting each droplet with multiple cells favors the evolution of
386 increased competitive ability.
387
388 *Tradeoff between competitive ability and numerical yield*
389 If competitive ability and numerical yield strictly traded off, then competitive ability would
390 decrease in the private-droplet treatment as numerical yield increased, and numerical yield would
391 decrease in the shared-droplet treatment as competitive ability increased. However, we did not see
392 such a strict tradeoff. Although the private-droplet descendants had larger gains in numerical yield,
393 some shared-droplet descendants also experienced moderate gains in numerical yield. Similarly,
394 although the shared-droplet descendants exhibited larger gains in competitive ability, some
395 private-droplet descendants also showed moderate improvements in their competitive ability.
396 Thus, these two traits do not strictly tradeoff with one another, and instead there seems to be some
397 misalignment, in which larger gains in one trait sometimes occur with more modest gains in the
398 other trait.
399 To develop this notion of misalignment further, we can contrast the case of a strict tradeoff,
400 or pure antagonistic pleiotropy (Figure 4a), with two different scenarios of synergistic pleiotropy.
401 The first synergistic scenario involves strict alignment, such that a mutation that is most beneficial
402 for trait 1 is also the most beneficial for trait 2 (Figure 4b). In essence, this scenario is the opposite
403 of strict antagonistic pleiotropy. The second form of synergism involves misalignment. In this
404 scenario, all mutations simultaneously improve both traits, but the mutations that are the strongest
405 for trait 1 are the weakest for trait 2, and *vice versa* (Figure 4c). Misalignment occurs when the
406 relative effect of a mutation on one trait is the opposite of its relative effect on another trait.
407 Therefore, antagonistic pleiotropy (Figure 4a) is also a case of misalignment, although the term is

broader than the traditional definition of "antagonism" (as illustrated in Figure 4c). In the Supplementary section, we develop a statistical test for misalignment. Using this test, we find that the increases in numerical yield in the private-droplet treatment came with concomitant weaker performance in competitive ability, while the improvements in competitive ability in the shared-droplet treatment came with weaker performance in numerical yield. Despite the absence of a strict tradeoff, these traits exhibited misalignment in our experiment. When two traits are misaligned, independent evolution in environments that favor one trait or the other can produce a pattern that supports a canonical tradeoff curve when the descendants are pooled across environments and the ancestors are ignored (i.e., considering only the colored points, while ignoring the grey points, in Figures 3 and 4c).

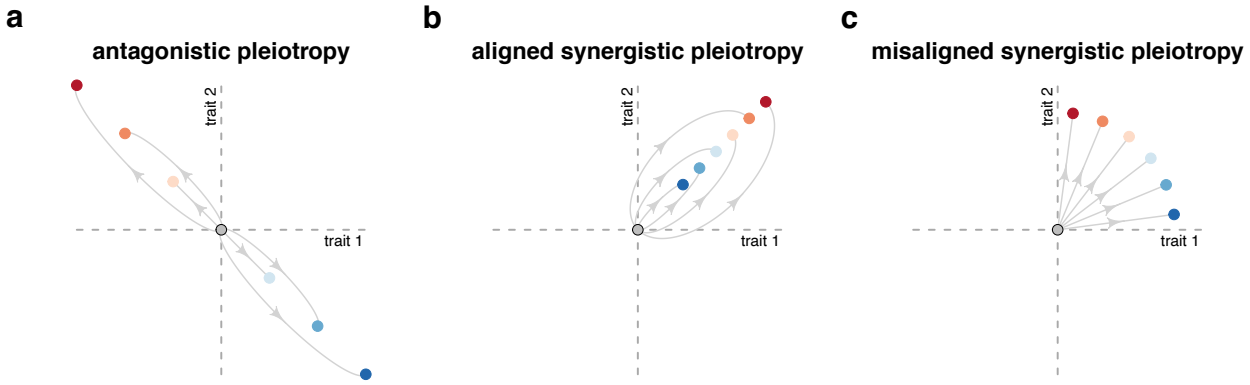

Figure 4: Three scenarios for pleiotropy with respect to two traits. The grey circle is the focal, ancestral genotype and the colored circles show the phenotypes of evolved genotypes. Here, fitness improvement with regard to a trait is taken to mean a *positive* change relative to the ancestor. (a) Antagonistic pleiotropy under a "strict tradeoff" situation, in which an improvement in one trait leads to a decline in the other, and the magnitude of enhancement in one dimension correlates with the magnitude of deterioration in the other. (b) Aligned synergistic pleiotropy describes a situation where the magnitude of improvement in one trait correlates with the magnitude of improvement in the other. (c) Misaligned synergistic pleiotropy describes a situation in which evolution improves both traits, but those genotypes with the strongest improvement in one trait have the weakest improvement in the other.

Private-droplet treatment favored smaller cells

While performing microscopy to assess droplet diameter (Supplemental Figures S8 & S9), we noticed variation in cell size across the emulsion treatments. The cells that had evolved in

private droplets appeared smaller than cells that had evolved in shared droplets. We therefore decided to investigate this trait systematically. Figure 5 shows the relationship between cell size and numerical yield.

Both cell size and total biomass increased in all 12 LTEE populations during selection for increased competitive ability for shared resources despite the fact that neither is directly a target of selection under those conditions (Grant et al. 2021, Lenski & Mongold, 2000). This increase in cell size can be seen in our data for the three time points that we sampled from the Ara–5 population, by comparing the values of the three grey points along the x-axis in Figure 5. For the emulsion evolved lines, the median cell volume decreased in all of the isolates from the private-droplet treatment, and the changes were significant in three cases (BK 437, BK 438, BK 441: $p < 0.01$, unpaired, two-tailed t-test). Using an emulsion protocol similar to our private-droplet treatment, Bachman *et al*. (2013) also reported observing an evolved decrease in cell size in *Lactococcus lactis*. They noted that propagation in an emulsion system could favor such a change because any mutant that distributed the same total amount of biomass into a greater number of smaller cells would be able to colonize more droplets each transfer. Our shared-droplet treatment provides an appropriate control for this inference. Indeed, the median cell size actually increased slightly in all three replicates of this treatment, and the change was significant in one case (BK 443: $p < 0.01$, unpaired, two-tailed t-test). The opposing directional changes in our two treatments indicates that neither the emulsion environment nor the transfer protocol (pooling all droplets and transferring only a fraction of cells to the next growth cycle, as shown in Figure 2a) was responsible for the consistently smaller cells seen in the private-droplet descendants. Instead, these findings support the hypothesis that smaller cells evolved in response to the reduced inter-genotype competition in the private-droplet treatment. When the 0K, 20K, and 60K lines are pooled, the

454 difference in cell size between the private-droplet and shared-droplet descendants is marginally
455 significant (p=0.051, paired one-tailed t-test; see Supplementary section *Statistical Analysis).*
456

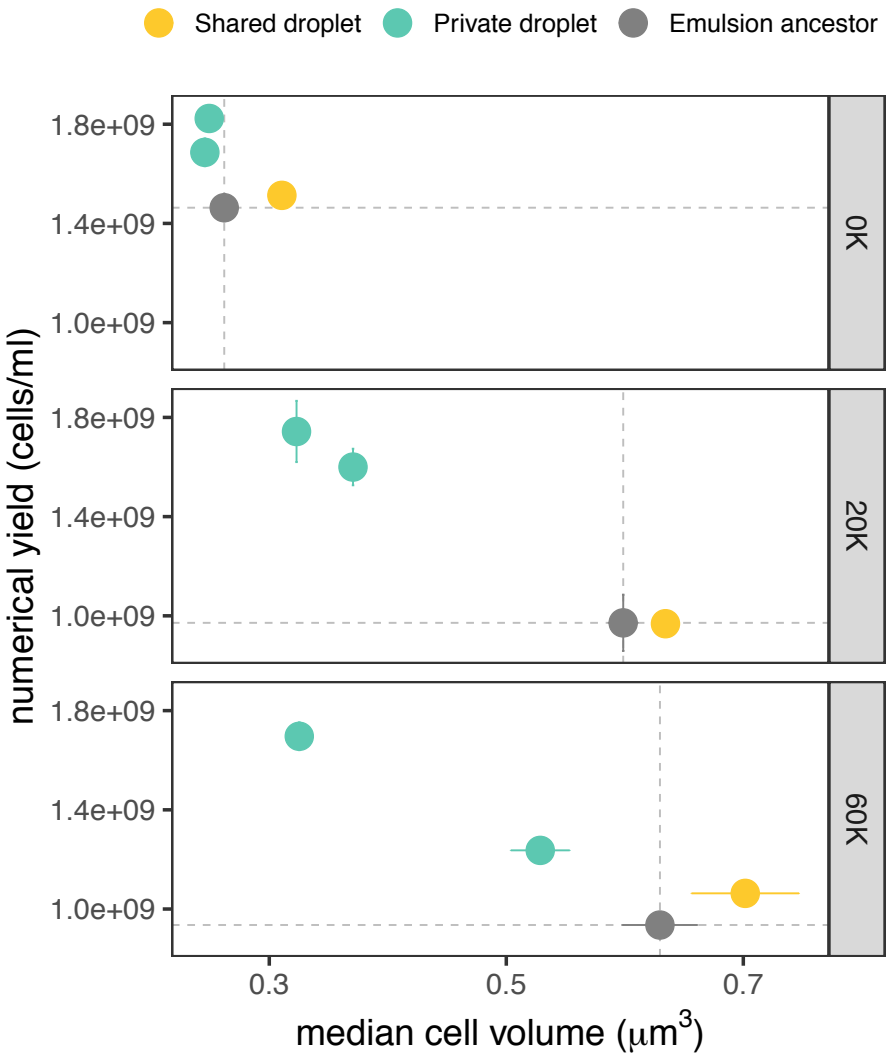

457

458 **Figure 5:** Median cell volume compared to numerical yield. Each panel shows strains originating from a single
459 emulsion ancestor (in grey, at right) from the Ara–5 lineage of the LTEE (0, 20,000, and 60,000 generations). Colors
460 indicate emulsion evolution treatments (labels at top). The coordinate positions of each point show the average of
461 three replicate assays for each phenotypic trait. Error bars show SEM; when they are not visible along either axis, the
462 corresponding SEM is smaller than the symbol itself. Dashed lines show the mean numerical yield and cell volume
463 of the relevant ancestor.

Genome sequencing reveals mutations in phosphoenolpyruvate phosphotransferase system

Given the evolution of smaller cells in the private-droplet treatment, we wondered if these populations were reverting to the ancestral state of the LTEE. After all, the progenitor of the LTEE (the 0K ancestor in our emulsion experiment) had very small cells. In particular, would the same genes and metabolic pathways that changed in the LTEE and led to larger cells in that experiment undergo reversion? Or would novel genetic and metabolic changes lead to a similar phenotypic endpoint? Also, would these changes depend on the particular LTEE-derived ancestor used in the emulsion experiment (e.g., 20K versus 60K)? To find out, we sequenced the complete genomes of 14 emulsion-evolved descendants and their three corresponding ancestors.

This whole-genome sequencing revealed a total number of 13 mutations that distinguish the evolved descendants from their ancestors (Table S4). We saw no cases of identical mutations in multiple descendants, nor was any gene mutated in descendants that evolved in the two different treatments. However, three of the six descendants from the private-droplet treatment had point mutations in genes encoding proteins in the phosphoenolpyruvate (PEP) phosphotransferase system (PTS) (Table 1), which is involved in glucose uptake (Carmona et al. 2015; Escalante et al. 2012; Nam et al. 2001; New et al. 2014; Notley-Mcrobb et al. 2006; Xia et al. 2017). All three of these descendants also had increased numerical yield and reduced cell size (Table S2), and all three were derived from the 20K and 60K emulsion ancestors. Of the three private-droplet descendants without mutations in PTS genes, two derived from the 0K ancestor, which already had high numerical yield in the emulsion conditions. The third private-droplet descendant without mutations in PTS genes derived from the 60K ancestor, and it exhibited much smaller changes in numerical yield and cell size than its counterpart with a PTS-associated mutation. The changes in numerical yield and cell size were also small for both of the private-droplet descendants derived

488 from the 0K ancestor, suggesting that the high-yield phenotype of the LTEE progenitor was largely
489 maintained. Bachmann et al. (2013) also found a point mutation in a PTS gene in one strain that
490 evolved increased numerical yield in emulsions, suggesting that PTS might have some role in
491 modulating numerical yield.

492 The PTS-associated mutations occurred in *ptsH*, which encodes a phosphocarrier protein;
493 *ptsG*, which encodes a subunit of the glucose transporter; and *crp*, which encodes a global
494 transcriptional regulator that affects some steps in glucose uptake (Kimata et al. 1997). Given that
495 these mutations include an early stop codon and non-conservative changes in amino acids, it is
496 likely that some or all of them cause reductions or even losses of function. Mutations in *pykF,*
497 which encodes pyruvate kinase, were among the earliest and most repeatable genetic changes in
498 the LTEE (Woods et al. 2006; Tenaillon et al. 2016; Peng et al. 2018). These mutations presumably
499 reduce the conversion of PEP to pyruvate in central metabolism, which would leave more PEP
500 available to power the transport of PTS-dependent sugars. Indeed, distinct patterns of pleiotropy
501 were observed in the LTEE for various substrates that differed in terms of whether their uptake
502 requires the PTS (Travisano & Lenski, 1996). Thus, although the mutations selected in the private
503 droplet-treatment were not in the same genes as those responsible for phenotypic changes in the
504 LTEE, they appear to affect the same system.
505

STRAIN (BK#)	LTEE GEN	POSITION	REF	ALT	ANNOTATION	GENE	DESCRIPTION
437	20K	2462747	A	C	*86Y (TAA→TAC)	*ptsH*	phosphocarrier protein Hpr
437	20K	3414187	G	A	E55K (GAA→AAA)	*crp*	cAMP-activated global transcriptional regulator CRP
438	20K	1173797	G	A	G454S (GGT→AGT)	*ptsG*	PTS glucose transporter subunit IIBC
441	60K	2462629	T	C	L47P (CTG→CCG)	*ptsH*	phosphocarrier protein Hpr

506 **Table 1:** Mutations in private-droplet descendants associated with PTS.

507

508 *Slower glucose uptake and decreased overflow metabolism in private-droplet descendants*

509 Perhaps the private-droplet descendants achieved their higher numerical yield and smaller
510 cell size in a physiologically similar way to the LTEE progenitor, despite genetic changes that did
511 not merely reverse those that occurred during the LTEE. Because the mutations we found in the
512 PTS system would be predicted to affect glucose transport, we decided to directly examine whether
513 the private-droplet descendants had evolved toward a metabolic state, at least in terms of glucose
514 use and overflow metabolite production, that resembled the LTEE progenitor.

515 We examined the concentrations of both glucose and various excreted metabolites in spent
516 medium as the various bacterial strains grew in emulsions (Figure 6a). We observed that the
517 glucose concentration for the 20K and 60K private-droplet descendants decreased more slowly
518 than for the corresponding shared-droplet descendants, their ancestors, and the 0K descendants of
519 either the shared or private droplets (Figure 6a, glucose panel). The slower glucose consumption
520 was most pronounced in the private-droplet descendants that had mutations in PTS, indicating that
521 these mutations likely simultaneously reduce the rate of glucose utilization while increasing
522 numerical yield.

523 The primary metabolite that is excreted by *E. coli* growing on glucose, and by the LTEE
524 lines in particular, is acetate (Harcombe et al. 2013). Acetate is a byproduct of both glycolysis and
525 fermentation, which is a less efficient form of metabolism than respiration (Szenk et al. 2017). The
526 0K emulsion evolution decedents did not markedly differ in metabolic signatures from the LTEE
527 ancestor. However, we saw differences in acetate production between the private-droplet
528 descendants from 20K and 60K and their emulsion ancestors. Specifically, the private-droplet
529 descendants produced less acetate, which suggests they were more efficient at glucose metabolism

under these conditions than their ancestor. In contrast, some of the shared-droplet descendants accumulated higher levels of acetate (Fig. 6a). In both cases, the acetate concentration eventually declines as it is consumed by the cells after they have depleted the available glucose. Interestingly, in emulsion-evolved populations of a different strain of *E. coli* (MG1655), Rabbers et al. (2021) found an increased numerical yield was achieved with no change in acetate production. Those results are consistent with our observations for the 0K descendants but differ from what we observe in the 20K and 60K descendants, which suggests a history of rate adaptation may leave its mark on future evolution.

In addition to acetate, other organic acids such as formate and lactate can be generated by *E. coli* during growth on glucose. For all of the isolates in our study, either formate or lactate was generated, but not both. For the 0K lineages, formate was produced by all types (ancestor, private-droplet descendants, and shared-droplet descendant). For the 20K and 60K lineages, only the shared-droplet descendant produced formate, whereas lactate was produced by the 20K and 60K ancestors and their private-droplet descendants.

Differences between strains in the accumulated concentrations of excreted metabolites might reflect different production rates, but they might also be influenced by differences in growth rate, as well as subsequent consumption of those products. We therefore standardized these measurements by computing the rate of production of each excreted metabolite per unit of glucose consumed, and by excluding time points after the remaining glucose fell below a threshold concentration (see *Methods—Analysis of metabolic data*). After so doing, Figure 6b shows a positive relationship between the initial rate of glucose utilization and the fraction of this carbon that is “wasted” as excreted metabolites in the 20K and 60K emulsion lines. Carbon waste was calculated as a sum of the concentrations across all excreted metabolites concentrations, weighted

by the number of carbon atoms in each metabolite. The data indicate that the shared-droplet descendants use the glucose rapidly, but in a relatively wasteful way, whereas the private-droplet descendants consume glucose more slowly and efficiently.

We used these standardized rates (Table S5) to perform a principal components analysis (PCA; Figure 6c) in order to visualize the differences between the emulsion ancestors and their descendants. The metabolic changes between the 0K ancestor and its descendants were modest, but the changes in the 20K and 60K lines were much greater. For the 20K and 60K ancestors, the metabolic shifts in the private-droplet treatment were distinct from those in the shared-droplet treatment, while the overall patterns of change were nearly identical for the 20K and 60K lines. Thus, in addition to PTS-related mutations conferring high numerical yield for three of the four private-droplet descendants of these two ancestors, the magnitude and nature of the metabolic changes appear similar. One private-droplet descendant (derived from the 60K ancestor) exhibited a smaller decrease in cell size and a more moderate increase in numerical yield (Figure 5). This isolate also did not have mutations associated with PTS, and it differed somewhat less in its metabolic profile from its ancestor. On balance, therefore, we lack clear support for either the Mutational Access Hypothesis or the Strength of Selection Hypothesis (Figure 1). Nonetheless, it is clear that just one or a few novel genetic changes can restore, at least approximately, the ancestral phenotypes of slow growth, small cells, and high numerical yield, even after tens of thousands of generations that led to faster growth, larger cells, and lower numerical yield.

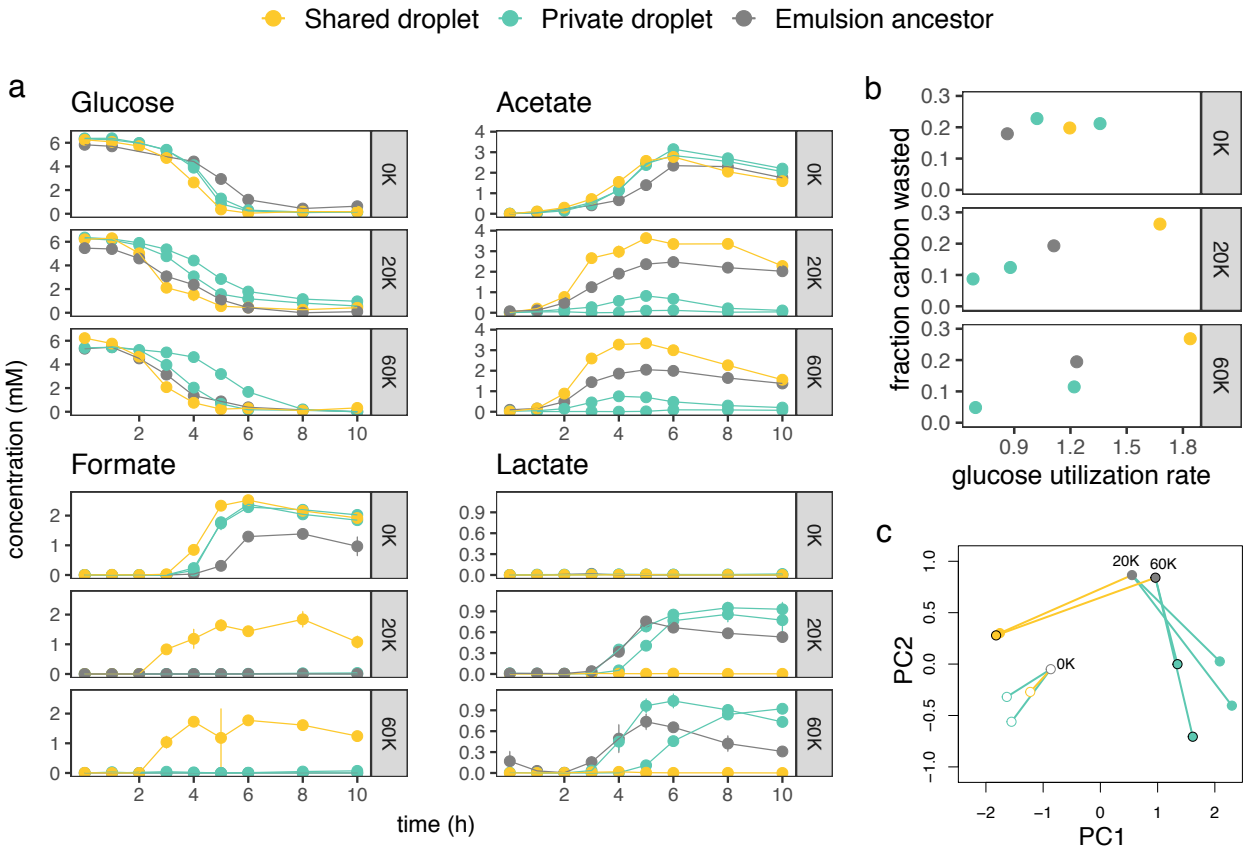

Figure 6: Glucose consumption and metabolite production. a) The concentrations of glucose, acetate, formate and lactate over 10 hours. Each trajectory shows one strain, and each point along a trajectory is the average of up to three replicates per strain. Colors indicate emulsion evolution treatments (labels at top). b) Glucose utilization versus the fraction of carbon wasted. c) Principal components analysis (PCA) based on the strain-specific rates of excreted metabolites per unit glucose consumed. The 0K strains are shown as empty points, the 20K strains as filled points without borders, and the 60K strains as filled points with borders. Lines, colored by treatment, connect emulsion ancestors (grey points) to their descendants.

Summary

Three of the four private-droplet descendants of the 20K and 60K ancestors achieved or even surpassed the numerical yield of the ultimate LTEE progenitor (the 0K emulsion ancestor). When compared to their ancestors, these high-yield descendants showed several parallel changes: smaller cells, more efficient glucose metabolism, mutations in genes encoding the PTS, and lower levels of acetate production. None of these changes occurred in the descendants that evolved from the same ancestors under the shared-droplet treatment. While the increased numerical yield and

588 smaller cell size appeared to be reversions to the phenotypic state of the ultimate progenitor, the
589 genetic and metabolic underpinnings of the descendants' phenotypes were distinct from those of
590 the ultimate progenitor. Specifically, mutations in genes encoding the PTS were not responsible
591 for evolutionary improvement in growth rate during the LTEE, and the metabolic profiles of the
592 20K and 60K private-droplet descendants were distinct from that of the 0K emulsion ancestor (Fig.
593 6c). Therefore, these data indicate a novel mechanistic basis for phenotypic reversion in this
594 system. Specifically, mutations in the PTS likely involved a reduction in glucose uptake, thereby
595 lowering the growth rate (and leading to a reduced competitive ability). However, these same
596 mutations appear to lead to both smaller size and limited loss of carbon via overflow metabolites,
597 thereby improving numerical yield. Notably, the same kind of mutations produced the phenotypic
598 reversion for both the 20K and 60K emulsion lines.

599 Dollo's law of irreversibility states that "An organism never returns exactly to a former
600 state, even if it finds itself placed in conditions of existence identical to those in which it has
601 previously lived. But by virtue of the indestructibility of the past [...] it always keeps some trace
602 of the intermediate stages through which it has passed" (Gould, 1970). Our experiment certainly
603 did not return these organisms to their ancestral conditions. However, the private-droplet treatment
604 was designed to place populations under selection for an ancestral phenotype, namely higher yield.
605 Even as the private-droplet lineages derived from later generations of the LTEE recovered the high
606 numerical yield of the LTEE ancestor, their phenotypic "return" did not involve a straightforward
607 reversal of the steps in their evolutionary history. Rather, the mutational targets and metabolic
608 patterns underlying their return were distinct from those evolutionary paths explored in the LTEE.
609 By contrast, when under the same selection for increased numerical yield, the private-droplet
610 descendants of the 0K emulsion ancestor exhibited genetic and metabolic changes distinct from

611 the 20K and 60K emulsion lines, suggesting that changes during the first 20,000 generations of
612 the LTEE had altered the potential for subsequent adaptation to the private-droplet regime Such
613 contingency is a recurring feature of adaptation in biological systems (Blount et al. 2008; Card et
614 al. 2019). However, we found no evidence of contingency in the later generations, as both the
615 intermediate (20K) and late (60K) isolates from the LTEE readily recovered their ancestral form,
616 seemingly by taking similar steps. Therefore, past evolution need not invariably alter future
617 evolution, even when the future involves a return to the past.
618
619
620
621
622
623
624
625
626
627
628
629
630
631

References

Agrawal, A. A., Conner, J. K., & Rasmann, S. (2010). Tradeoffs and Negative Correlationsin Evolutionary Ecology BT - Evolution Since Darwin. *Evolution Since Darwin*, (10), 243–268.

Bachmann, H., M. Fischlechner, I. Rabbers, N. Barfa, F. Branco dos Santos, D. Molenaar, and B. Teusink. 2013. "Availability of Public Goods Shapes the Evolution of Competing Metabolic Strategies." *Proceedings of the National Academy of Sciences* 110(35):14302–7. doi: 10.1073/pnas.1308523110.

Barrick, J E, and Lenski, R. E. "Genome-wide mutational diversity in an evolving population of Escherichia coli." *Cold Spring Harbor symposia on quantitative biology* vol. 74 (2009): 119-29. doi:10.1101/sqb.2009.74.018

Barrick, J. E., Kauth, M. R., Strelioff, C. C., & Lenski, R. E. (2010). Escherichia coli rpoB mutants have increased evolvability in proportion to their fitness defects. *Molecular Biology and Evolution*, *27*(6), 1338–1347. https://doi.org/10.1093/molbev/msq024

Beardmore, R. E., Gudelj, I., Lipson, D. A., & Hurst, L. D. (2011). Metabolic trade-offs and the maintenance of the fittest and the flattest. *Nature*, *472*(7343), 342–346. https://doi.org/10.1038/nature09905

Blount, Z. D., C. Z. Borland, and Lenski, R. E. 2008. Historical contingency and the evolution of a key innovation in an experimental population of *Escherichia coli*. *Proceedings of the National Academy of Sciences, USA* 105: 7899-7906.

Card, K. J., T. LaBar, J. B. Gomez, and Lenski, R. E. 2019. Historical contingency in the evolution of antibiotic resistance after decades of relaxed selection. *PLOS Biology* 17: e3000397.

Carmona, S. B., Moreno, F., Bolívar, F., Gosset, G., & Escalante, A. (2015). Inactivation of the PTS as a Strategy to Engineer the Production of Aromatic Metabolites in Escherichia coli. *Journal of Molecular Microbiology and Biotechnology*, *25*(2–3), 195–208. https://doi.org/10.1159/000380854

Chou, H. H., Chiu, H. C., Delaney, N. F., Segrè, D., & Marx, C. J. (2011). Diminishing returns epistasis among beneficial mutations decelerates adaptation. *Science*, *332*(6034), 1190–1192. https://doi.org/10.1126/science.1203799

Deatherage D.E., Barrick J. E. 2014. "Identification of Mutations in Laboratory-Evolved Microbes from Next-Generation Sequencing Data Using Breseq. In: Sun L., Shou W. (Eds) Engineering and Analyzing Multicellular Systems. Methods in Molecular Biology (Methods and Protocols)." 1151:1–22. doi: 10.1007/978-1-4939-0554-6.

673 Escalante, A., Cervantes, A. S., Gosset, G., & Bolívar, F. (2012). Current knowledge of the
674 Escherichia coli phosphoenolpyruvate-carbohydrate phosphotransferase system:
675 Peculiarities of regulation and impact on growth and product formation. *Applied*
676 *Microbiology and Biotechnology*, *94*(6), 1483–1494. https://doi.org/10.1007/s00253-012-
677 4101-5

678 Eshelman, C. M., Vouk, R., Stewart, J. L., Halsne, E., Lindsey, H. a, Schneider, S., … Kerr, B.
679 (2010). Unrestricted migration favours virulent pathogens in experimental metapopulations:
680 evolutionary genetics of a rapacious life history. *Philosophical Transactions of the Royal*
681 *Society of London. Series B, Biological Sciences*, *365*, 2503–2513.
682 https://doi.org/10.1098/rstb.2010.0066

683 Farmer, I. S., & Jones, C. W. (1976). The Energetics of Escherichia coli during Aerobic Growth
684 in Continuous Culture. *European Journal of Biochemistry*, *67*(1), 115–122.
685 https://doi.org/10.1111/j.1432-1033.1976.tb10639.

686 Gould, S. J. (1970). Dollo on Dollo ' s Law : Irreversibility and the Status of Evolutionary Laws
687 Author (s): Stephen Jay Gould Source : Journal of the History of Biology , Vol . 3 , No . 2
688 (Autumn , 1970), pp . 189-212 Published by : Springer Stable URL : http://www.jsto. *J*
689 *Hist Biol.*, *3*(2), 189–212.
690
691 Gounand, I., Daufresne, T., Gravel, D., Bouvier, C., Bouvier, T., Combe, M., … Mouquet, N.
692 (2016). Size evolution in microorganisms masks trade-offs predicted by the growth rate
693 hypothesis. *Proceedings of the Royal Society B: Biological Sciences*, *283*(1845), 20162272.
694 https://doi.org/10.1098/rspb.2016.2272
695
696 Grant, N. A., Abdel Magid, A., Franklin, J., Dufour, Y., & Lenski, R. E. (2021). Changes in Cell
697 Size and Shape During 50,000 Generations of Experimental Evolution with Escherichia
698 coli. *Journal of Bacteriology*, (March). https://doi.org/10.1128/jb.00469-20
699
700 Guillaume, F., & Otto, S. P. (2012). Gene functional trade-offs and the evolution of pleiotropy.
701 *Genetics*, *192*(4), 1389–1409. https://doi.org/10.1534/genetics.112.143214
702
703 Harcombe, W. R., Delaney, N. F., Leiby, N., Klitgord, N., & Marx, C. J. (2013). The Ability of
704 Flux Balance Analysis to Predict Evolution of Central Metabolism Scales with the Initial
705 Distance to the Optimum. *PLoS Computational Biology*, *9*(6).
706 https://doi.org/10.1371/journal.pcbi.1003091

707 Johnston, G. C., Ehrhardt, C. W., Lorincz, A., & Carter, B. L. A. (1979). Regulation of cell size
708 in the yeast Saccharomyces cerevisiae. *Journal of Bacteriology*, *137*(1), 1–5.
709 https://doi.org/10.1128/jb.137.1.1-5.1979

710 Kerr, B., Neuhauser, C., Bohannan, B. J. M., & Dean, A. M. (2006). Local migration promotes
711 competitive restraint in a host-pathogen "tragedy of the commons." *Nature*, *442*(7098), 75–
712 78. https://doi.org/10.1038/nature04864
713

714 Kimata, K., Takahashi, H., Inada, T., Postma, P., & Aiba, H. (1997). cAMP receptor protein-
715 cAMP plays a crucial role in glucose-lactose diauxie by activating the major glucose
716 transporter gene in Escherichia coli. *Proceedings of the National Academy of Sciences of*
717 *the United States of America*, *94*(24), 12914–12919.
718 https://doi.org/10.1073/pnas.94.24.12914
719
720 Leiby, N., Harcombe, W. R., & Marx, C. J. (2012). Multiple long-term, experimentally-evolved
721 populations of Escherichia coli acquire dependence upon citrate as an iron chelator for
722 optimal growth on glucose. *BMC Evolutionary Biology*, *12*(1).
723 https://doi.org/10.1186/1471-2148-12-151

724 Leiby, N., & Marx, C. J. (2014). Metabolic Erosion Primarily Through Mutation Accumulation,
725 and Not Tradeoffs, Drives Limited Evolution of Substrate Specificity in Escherichia coli.
726 *PLoS Biology*, *12*(2). https://doi.org/10.1371/journal.pbio.1001789

727 Lenski, R. E. 2017. "Experimental Evolution and the Dynamics of Adaptation and Genome
728 Evolution in Microbial Populations." *The ISME Journal* 1–14. doi: 10.1038/ismej.2017.69.

729 Lenski, R. E., and Travisano, M. 1994. "Dynamics of Adaptation and Diversification: A 10,000-
730 Generation Experiment with Bacterial Populations." *Proceedings of the National Academy*
731 *of Sciences of the United States of America* 91(15):6808–14. doi: 10.1073/pnas.91.15.6808.
732
733 Levin, B. R., Lipsitch, M., Perrot, V., Schrag, S., Antia, R., Simonsen, L., … Stewart, F. M.
734 (1997). The population genetics of antibiotic resistance. *Clinical Infectious Diseases : An*
735 *Official Publication of the Infectious Diseases Society of America*, *24 Suppl 1*, S9-16.
736 Retrieved from http://www.ncbi.nlm.nih.gov/pubmed/8994776
737
738 Manhart, M., Adkar, B. V., & Shakhnovich, E. I. (2016). *Tradeoffs between microbial growth*
739 *phases lead to frequency-dependent and non-transitive selection*.
740 https://doi.org/http://dx.doi.org/10.1101/096453

741 Monds, R. D., Lee, T. K., Colavin, A., Ursell, T., Quan, S., Cooper, T. F., & Huang, K. C.
742 (2014). Systematic Perturbation of Cytoskeletal Function Reveals a Linear Scaling
743 Relationship between Cell Geometry and Fitness. *Cell Reports*, *9*(4), 1528–1537.
744 https://doi.org/10.1016/j.celrep.2014.10.040

745 Mongold, J. A., and Lenski, R. E. 1996. Experimental rejection of a nonadaptive explanation for
746 increased cell size in *Escherichia coli*. *Journal of Bacteriology* 178: 5333-5334.

747 Nam, T. W., Cho, S. H., Shin, D., Kim, J. H., Jeong, J. Y., Lee, J. H., … Seok, Y. J. (2001). The
748 Escherichia coli glucose transporter enzyme IICBGlc recruits the global repressor Mlc.
749 *EMBO Journal*, *20*(3), 491–498. https://doi.org/10.1093/emboj/20.3.491

750 New, A. M., Cerulus, B., Govers, S. K., Perez-Samper, G., Zhu, B., Boogmans, S., …
751 Verstrepen, K. J. (2014). Different Levels of Catabolite Repression Optimize Growth in

752 Stable and Variable Environments. *PLoS Biology*, *12*(1), 17–20.
753 https://doi.org/10.1371/journal.pbio.1001764

754 Notley-McRobb, L., Death, A., & Ferenci, T. (2006). The relationship between external glucose
755 concentration and cAMP levels inside. *Biochemical Journal*, (1997), 1909–1918.
756 https://doi.org/10.1099/00221287-143-6-1909

757 Novak, M., Pfeiffer, T., Lenski, R. E., Sauer, U., & Bonhoeffer, S. (2006). Experimental tests for
758 an evolutionary trade-off between growth rate and yield in E. coli. *The American Naturalist*,
759 *168*(2), 242–251. https://doi.org/10.1086/506527

760 Pavličev, M., & Cheverud, J. M. (2015). Constraints Evolve: Context Dependency of Gene
761 Effects Allows Evolution of Pleiotropy. *Annual Review of Ecology, Evolution, and*
762 *Systematics*, *46*(1), 413–434. https://doi.org/10.1146/annurev-ecolsys-120213-091721
763
764 Peng, F., Widmann, S., Wünsche, A., Duan, K., Donovan, K. A., Dobson, R. C. J., … Cooper, T.
765 F. (2018). Effects of Beneficial Mutations in pykF Gene Vary over Time and across
766 Replicate Populations in a Long-Term Experiment with Bacteria. *Molecular Biology and*
767 *Evolution*, *35*(1), 202–210. https://doi.org/10.1093/molbev/msx279
768
769 Pennings, P. S., Ogbunugafor, C. B., & Hershberg, R. (2020). Reversion is most likely under
770 high mutation supply, when compensatory mutations don't fully restore fitness costs.
771 *BioRxiv*. https://doi.org/10.1101/2020.12.28.424568

772 Pfeiffer, T., Schuster, S., & Bonhoeffer, S. (2001). *Cooperation and Competition in the*
773 *Evolution of ATP-Producing Pathways*. *292*(April).

774 Pierucci, O. (1978). Dimensions of Escherichia coli at various growth rates: model for envelope
775 growth. *Journal of Bacteriology*, *135*(2), 559–574.

776 Ostrowski, E. A., Ofria, C., & Lenski, R. E. (2015). Genetically integrated traits and rugged
777 adaptive landscapes in digital organisms Experimental evolution. *BMC Evolutionary*
778 *Biology*, *15*(1), 1–14. https://doi.org/10.1186/s12862-015-0361-x

779 Quandt, E. M., Gollihar, J., Blount, Z. D., Ellington, A. D., Georgiou, G., & Barrick, J. E.
780 (2015). Fine-tuning citrate synthase flux potentiates and refines metabolic innovation in the
781 lenski evolution experiment. *ELife*, *4*(OCTOBER2015), 1–22.
782 https://doi.org/10.7554/eLife.09696

783 Rabbers, I., Gottstein, W., Feist, A., Teusink, B., & Bruggeman, F. J. (2021). Selection for cell
784 yield does not reduce overflow metabolism in E. coli. *BioRxiv*, 2021.05.24.445453.
785 Retrieved from https://doi.org/10.1101/2021.05.24.445453

786 Robinson, J. T., Thorvaldsdóttir, H., Winckler, W., Guttman, M., Lander, E. S., Getz, G., &
787 Mesirov, J. P. (2011). Integrative Genomics Viewer. *Nature Biotechnology*, *29*(1), 24–26.
788 https://doi.org/10.1038/nbt0111-24

789 Rose, M. (1982). *Antagonistic pleiotropy, dominance, and genetic variation*. 48*(2501).
790
791 Rose, M. R. (1985). Life history evolution with antagonistic pleiotropy and overlapping
792 generations. *Theoretical Population Biology*, *28*(3), 342–358. https://doi.org/10.1016/0040-
793 5809(85)90034-6
794
795 Schank, J., & Wimsatt, W. (2011). *Generative Entrenchment and Evolution Author (s): Jeffrey*
796 *C . Schank and William C . Wimsatt Source : PSA : Proceedings of the Biennial Meeting of*
797 *the Philosophy of Science Association , Vol . 1986 , Volume Two : Symposia and Invited*
798 *Papers (1986), pp. 1986*(1986), 33–60.
799
800 Shah, P., McCandlish, D. M., & Plotkin, J. B. (2015). Contingency and entrenchment in protein
801 evolution under purifying selection. *Proceedings of the National Academy of Sciences of the*
802 *United States of America*, *112*(25), E3226–E3235. https://doi.org/10.1073/pnas.1412933112
803
804 Stearns, S. C. 1989. "Trade-Offs in Life-History Evolution Published by: British Ecological
805 Society Stable URL: Https://Www.Jstor.Org/Stable/2389364 Trade-Offs in Life-History
806 Evolution." *Functional Ecology* 3(3):259–68.
807
808 Stevenson, K., McVey, A. F., Clark, I. B. N., Swain, P. S., & Pilizota, T. (2016). General
809 calibration of microbial growth in microplate readers. *Scientific Reports*, *6*(December), 4–
810 10. https://doi.org/10.1038/srep38828

811 Szenk, M., Dill, K. A., & de Graff, A. M. R. (2017). Why Do Fast-Growing Bacteria Enter
812 Overflow Metabolism? Testing the Membrane Real Estate Hypothesis. *Cell Systems*, *5*(2),
813 95–104. https://doi.org/10.1016/j.cels.2017.06.005

814 Tenaillon, O., J. E. Barrick, N. Ribeck, D. E. Deatherage, J. L. Blanchard, A. Dasgupta, G. C.
815 Wu, S. Wielgoss, S. Cruveiller, C. Médigue, D. Schneider, and R. E. Lenski. 2016. Tempo
816 and mode of genome evolution in a 50,000-generation experiment. *Nature* 536: 165-170.

817 Teotónio, H., & Rose, M. R. (2000). Variation in the reversibility of evolution. *Nature*,
818 *408*(6811), 463–466. https://doi.org/10.1038/35044070

819 Travisano, M., and R. E. Lenski. 1996. "Long-Term Experimental Evolution in Escherichia Coli.
820 IV. Targets of Selection and the Specificity of Adaptation." *Genetics* 143(1):15–26. doi:
821 10.1007/s000360050052.
822
823 van Tatenhove-Pel, R. J., Zwering, E., Boreel, D. F., Falk, M., van Heerden, J. H., Kes, M. B. M.
824 J., … Bachmann, H. (2021). Serial propagation in water-in-oil emulsions selects for
825 Saccharomyces cerevisiae strains with a reduced cell size or an increased biomass yield on
826 glucose. *Metabolic Engineering*, *64*(November 2020), 1–14.
827 https://doi.org/10.1016/j.ymben.2020.12.005
828

Vasi, F., Travisano, M., & Lenski, R. E. (1994). Long-Term Experimental Evolution in Escherichia coli . II . Changes in Life-History Traits During Adaptation to a Seasonal Environment. *The University of Chicago Press 144*(3), 432–456.

Velicer, G. J. (1999). Pleiotropic effects of adaptation to a single carbon source for growth on alternative substrates. *Applied and Environmental Microbiology*, *65*(1), 264–269. https://doi.org/10.1128/aem.65.1.264-269.1999

Wiser, M. J., Ribeck, N., and Lenski, R. E. 2013. "Long-Term Dynamics of Adaptation in Asexual Populations." *Science (New York, N.Y.)* 342(6164):1364–67. doi: 10.1126/science.1243357.

Woods, R. J., Barrick, J. E., Cooper, T. F., Shrestha, U., Kauth, M. R., & Lenski, R. E. (2011). *Second-Order Selection for Evolvability in a Large Escherichia coli Population*. (March), 1433–1437.

Woods, R., D. Schneider, C. L. Winkworth, M. A. Riley, and Lenski, R. E. (2006). Tests of parallel molecular evolution in a long-term experiment with *Escherichia coli*. *Proceedings of the National Academy of Sciences, USA* 103:9107-9112.

Xia, T., Sriram, N., Lee, S. A., Altman, R., Urbauer, J. L., Altman, E., and Eiteman, M. A. 2017. "Glucose Consumption in Carbohydrate Mixtures by Phosphotransferase-System Mutants of Escherichia Coli." *Microbiology (United Kingdom)* 163(6):866–77. doi: 10.1099/mic.0.000480.

Yulo, P. R. J., & Hendrickson, H. L. (2019). The evolution of spherical cell shape; progress and perspective. *Biochemical Society Transactions*, *47*(6), 1621–1634. https://doi.org/10.1042/BST20180634

875
876
877
878